Recent advances in non-invasive magnetic resonance imaging assessment of hepatocellular carcinoma

Davide Ippolito, Riccardo Inchingolo, Luigi Grazioli, Silvia Girolama Drago, Michele Nardella, Marco Gatti, Riccardo Faletti

Davide Ippolito, Silvia Girolama Drago, School of Medicine, University of Milano-Bicocca, Milan 20126, Italy

Davide Ippolito, Silvia Girolama Drago, Department of Diagnostic Radiology, HS Gerardo Monza, Monza (MB) 20900, Italy

Riccardo Inchingolo, Michele Nardella, Division of Interventional Radiology, Department of Radiology, Madonna delle Grazie Hospital, Matera 75100, Italy

Marco Gatti, Riccardo Faletti, Department of Surgical Sciences, Radiology Unit, University of Turin, Turin 10126, Italy

Luigi Grazioli, Department of Radiology, University of Brescia "Spedali Civili", Brescia 25123, Italy

ORCID number: Davide Ippolito (0000-0002-2696-7047); Riccardo Inchingolo (0000-0002-0253-5936); Luigi Grazioli (0000-0002-2345-1571); Silvia Girolama Drago (0000-0003-3569-2118); Michele Nardella (0000-0002-1573-511X); Marco Gatti (0000-0001-8168-5280); Riccardo Faletti (0000-0002-8865-8637).

Author contributions: All authors equally contributed to this paper with conception and design of the study, literature review and analysis, drafting and critical revision and editing, and final approval of the final version.

Conflict-of-interest statement: All the authors are aware of the content of the manuscript and have no conflict of interest.

Manuscript source: Invited manuscript

Correspondence to: Davide Ippolito, MD, Adjunct Professor, Staff Physician, Department of Diagnostic Radiology, San Gerardo Hospital, University of Milano-Bicocca, Via Pergolesi 33, Monza (MB) 20900, Italy. davide.atena@tiscalinet.it
Telephone: +39-2-64488265
Fax: +39-2-64488299

Abstract

Magnetic resonance (MR) imaging of the liver is an important tool for the detection and characterization of focal liver lesions and for assessment of diffuse liver disease, having several intrinsic characteristics, represented by high soft tissue contrast, avoidance of ionizing radiation or iodinated contrast media, and more recently, by application of several functional imaging techniques (*i.e.*, diffusion-weighted sequences, hepatobiliary contrast agents, perfusion imaging, magnetic resonance (MR)-elastography, and radiomics analysis). MR functional imaging techniques are extensively used both in routine practice and in the field of clinical and pre-clinical research because, through a qualitative rather than quantitative approach, they can offer valuable information about tumor tissue and tissue architecture, cellular biomarkers related to the hepatocellular functions, or tissue vascularization profiles related to tumor and tissue biology. This kind of approach offers *in vivo* physiological parameters, capable of evaluating physiological and pathological modifications of tissues, by the analysis of quantitative data that could be used in tumor detection, characterization, treatment

selection, and follow-up, in addition to those obtained from standard morphological imaging. In this review we provide an overview of recent advanced techniques in MR for the diagnosis and staging of hepatocellular carcinoma, and their role in the assessment of response treatment evaluation.

Key words: Liver; Cirrhosis; Hepatocellular carcinoma; Magnetic resonance; Transarterial chemoembolization; Contrast media

Core tip: Magnetic resonance (MR) of the liver is an important diagnostic option for detection and characterization of focal liver lesions. To date, beside the standard morphological sequences, new functional imaging tools (*i.e.*, diffusion-weighted sequences, hepatobiliary contrast agents, perfusion imaging, MR-elastography, or radiomics analysis) have been introduced in clinical practice. The aim of functional imaging is to provide *in vivo* quantitative complementary functional data related to the tissue or tumor modifications, offering useful comprehensive information about the biology, behavior, and prognosis of hepatocellular carcinoma lesions. This functional approach may help clinicians correctly manage cirrhotic patients, also after therapeutic treatment.

INTRODUCTION

Liver cancer is the fifth most frequently diagnosed malignancy among men and the ninth among women. Recently, it has risen from the third to the second cause of death from cancer, accounting for nearly 746000 deaths in 2012. In some regions, like Eastern and South-Eastern Asia, mortality almost equals incidence with an overall ratio of 0.95[1]. The most common histological subtype of liver cancer is hepatocellular carcinoma (HCC), representing more than 90% of cases. The incidence of HCC increases with advanced age, reaching, at least in developed countries, a peak at 70 years[2]. In up to 90% of cases, HCC occurs in the setting of liver cirrhosis and overall, one-third of cirrhotic patients will develop HCC during their lifetimes[3].

The primary risk factor for HCC is still represented by chronic hepatitis B virus (HBV) or hepatitis C virus (HCV) infection[4], with a prevalence of virus B infection in Eastern countries and a prevalence of virus C infection in Western countries. Other causes of cirrhosis comprise

alcohol abuse, non-alcoholic fatty liver disease (NAFLD), and less frequent disorders such as hemochromatosis. All etiologies could lead to cirrhosis and may be complicated by tumor formation, but the risk is higher in patients with hepatitis infection. In the coming years, the diffusion of new antiviral agents for HCV[5], vaccination and therapy for HBV[6], and prevention campaigns are expected to reduce the burden of chronic viral liver disease and its complications, including HCC[7]. On the other hand, the widespread epidemic of obesity is expected to induce a significant increase in the incidence of NAFLD and its complications, such as NASH, cirrhosis, and HCC[8,9].

Liver cirrhosis is a common underlying condition associated with hepatocarcinogenesis. Cirrhosis develops after a long period of chronic liver disease, when the risk of HCC is still low. The nodules that could be potentially found in a cirrhotic liver comprise: Small and large regenerative nodule (RN), low-grade dysplastic nodule (LGDN), high-grade dysplastic nodule (HGDN), early HCC, well-differentiated HCC, and moderately-poorly differentiated HCC. Hepatocarcinogenesis is a multistep event during which cell density increases, Kuppfer cells decrease, nodules enlarge, and hemodynamics change. In the initial phase, normal arterial supply decreases but portal perfusion is still present. Later, intranodular arterial vascularity increases due to the appearance of unpaired arteries (capillarization) while portal blood supplies progressively decrease[10]. Simultaneously, organic anionic transporting polypeptide (OATP), transporters of bile salts, gradually decrease. OATP expression levels are high in RNs and LGDNs and lower in many HGDNs, early HCCs, and progressed HCCs. The hemodynamic changes are well depicted during dynamic multidetector computed tomography (MDCT) and magnetic resonance imaging (MRI), and both European and American guidelines have endorsed this technique for the diagnosis of HCC > 1 cm, based on the typical hallmarks of hypervascularity in arterial phase with wash-out in portal phase, thereby avoiding liver biopsy[11,12].

However, there remains a high rate of false negative, ranging from 25%-30%, in particular for nodules < 2 cm[13,14], which actually are the most often encountered focal liver lesions, thanks to the widespread of surveillance programs. In these small nodules, hemodynamic changes of hepatocarcinogenesis are in an early stage, since neoangiogenesis is incomplete and they are still mainly filled by portal vessels, in contrast to progressed HCC. MRI in part overcomes these limits. It has been recently demonstrated that this diagnostic technique has a higher diagnostic performance over computed tomography (CT) in the detection of high-risk nodules[15]. This is due to its high contrast resolution and to its multiparametric characteristics. In fact, it is known that hyperintensity on T2 weighted sequences and restricted diffusion in diffuse weighted images (DWI) are features of malignancy[16]. Moreover the recent introduction of hepatospecific MRI contrast agent
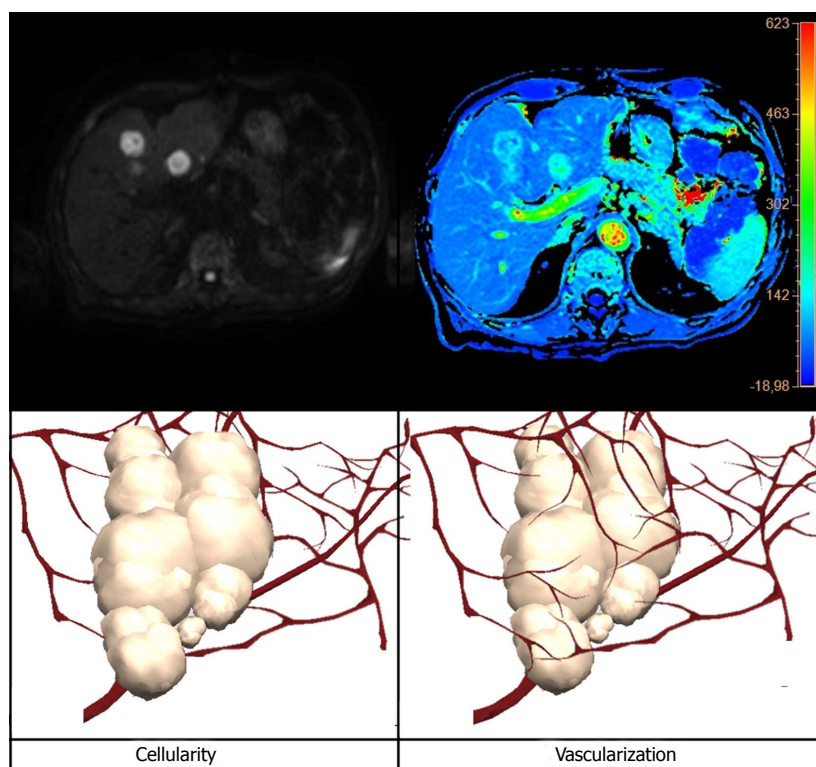
Figure 1 Schematic comparison between diffusion weighted images (on the left) and perfusion maps (on the right) showing the meaning from the pathophysiological point of view of the two different functional magnetic resonance techniques. The diffusion offers qualitative information strictly related to tissue cellularity, while perfusion sequences offer qualitative information about tissue vascularization.

gadolinium-ethoxybenzyl-dieth-ylenetriamine pentaacetic acid (Gd-EOB-DTPA, Primovist®; Bayer Schering Pharma, Berlin, Germany), which gives information not only on vascular changes but also on hepatocyte function, raises the sensitivity for the detection of early HCC to 91%-93%[17]. Based on this feature, Kim BR and colleagues[16] demonstrated that readers had significantly higher detection sensitivity for early HCCs with MRI than with multidetector CT (78.6% *vs* 52.4%, *P* = 0.001; 71.4% *vs* 50.0%, *P* = 0.011; and 73.8% *vs* 50.0%, *P* = 0.001, respectively), as shown by 30 more LI-RADS category 4 early HCCs identified at MRI.

The correct characterization of all nodules possibly encountered in a cirrhotic liver is of paramount importance because they are managed completely differently. In fact, while regenerative and dysplastic nodules deserve a strict follow-up, HCC should be treated with the more suitable therapeutic option, according its stage. This is clearly defined by the Barcelona Clinic Liver Cancer (BCLC) staging system, adopted in all Western countries and endorsed by both American and European guidelines.

In this context, beside traditional radiological techniques, new functional imaging tools have been introduced in clinical practice in order to provide not only morphological information but also functional data information. Functional magnetic resonance imaging encompasses a wide range of advanced techniques capable of evaluating physiological and pathological

modifications of tissues, by the analysis of quantitative data, in addition to those obtained from standard morphological imaging. These techniques may include diffusion-weighted sequences, hepatobiliary contrast agents, perfusion imaging, MR-elastography, and more recently radiomics analysis. In particular, perfusion imaging (related to vascular profile) and diffusion imaging (related to cellular profile) (Figure 1) techniques have been extensively studied during various steps of HCC evolution, from initial assessment of vascular modifications in cirrhotic liver, through its progression in tumor lesion, and finally to its follow-up after treatment. Hence, in this review, we provide an overview of recent advances and techniques in MR studies for the diagnosis and the staging of HCC.

CONTRAST MEDIA: EXTRACELLULAR AND HEPATOBILIARY AGENTS

Gadolinium is a paramagnetic ion that shortens T1 relaxation time in tissues and, therefore, produces an increase in signal intensity[18]. Based on bio-distribution, there are three categories of gadolinium-based contrast agents: extracellular fluid agents (ECFAs), blood pool agents (BPCAs), and targeted and organ-specific contrast agents, such as hepatocyte-specific contrast agents (HCAs). ECFAs and HCAs are the most commonly used in liver imaging. ECFAs consist of gadolinium chelated to an organic compound, such as DTPA[19]. They are

Table 1 Gadolinium-based magnetic resonance imaging contrast agent

Contrast agent	Category	Relaxivity	Structure	Concentration (mmol/mL)	Reccomended dosage (mmol/kg)
Gadoterate-meglumine	ECFAs	Standard	macrocyclic	0.5	0.1
Gadobutrol	ECFAs	Standard	macrocyclic	1.0	0.1
Gadoteridol	ECFAs	Standard	macrocyclic	0.5	0.1
Gadopentetate- dimeglumine	ECFAs	Standard	Linear	0.5	0.1
Gadoversetamide	ECFAs	Standard	Linear	0.5	0.1
Gadodiamide	ECFAs	Standard	Linear	0.5	0.1
Gadofosfaset-trisodium	BPCAs	High	Linear	0.25	0.03
Gadobenate- dimeglumine	HCAs	High	Linear	0.5	0.1
Gadoxetate-disodium	HCAs	High	Linear	0.25	0.025

ECFAs: Extracellular fluid agents; BPCAs: Blood pool agents; HCAs: Hepatocyte-specific contrast agents.

further divided in standard relaxivity macrocyclic agents, standard relaxivity linear agents, and high relativity linear agents (Table 1). The details regarding the advantages and disadvantages of each contrast category is beyond the scope of this article, but in general, there is little clinical difference[20]. The standard dose is 0.1 mmol/kg typically injected intravenously at a rate of 2 mL/s followed by a normal saline "flush" of 20 to 50 mL. After the injection, ECFAs are rapidly cleared from the intravascular space through the capillaries into the extracellular space. They are mainly eliminated by renal excretion and have imaging dynamics comparable to the extracellular iodinated contrast media used in CT. However, MRI is more sensitive to the effects of gadolinium than CT is to the effects of iodine, because gadolinium has an amplification effect due to the number of adjacent water protons relaxed by a single gadolinium atom[19,21]. In summary, ECFAs enter into the liver through the hepatic artery and portal vein and are freely redistributed into the interstitial space; they demonstrate vascular perfusion by distributing and allow the evaluation of liver lesions based on assessment of vascularity. The combination of arterial phase hyperenhancement followed by washout appearance in the portal venous and/or delayed phase is the key diagnostic feature of HCC[11,12] (Figure 2).

The pathophysiologic basis for arterial phase hyperenhancement in HCC is related to the increasing of the intranodular arterial supply during hepato-carcinogenesis[22]. The mechanisms underlying washout appearance in HCC depend on a range of factors: early venous drainage of contrast material from the tumor, progressive enhancement of background liver, reduced intranodular portal venous blood supply, tumor hypercellularity with corresponding reduction in extracellular volume, and intrinsic hypoattenuation/hypointensity[23]. In cirrhotic patients, this enhancement pattern has approximately 100% specificity for lesions larger than 2 cm and approximately 90% specificity for those of 1-2 cm[24]. However, the main limitation with ECFAs for diagnosis and staging HCCs is low per-lesion sensitivity, because an atypical vascular behavior is quite common in small (< 2 cm) nodules and approximately one-third of these are malignant

("the one-third rule")[25]. Indeed, the intranodular hemodynamic changes during carcinogenesis start with an arterial hypovascularity with portal perfusion still present, followed by a decrease of both arterial and portal blood supply, then followed by an increase in arterial vascularity to isovascular, and, finally, to a hypervascular pattern[12].

On the other hand, several recent studies demonstrated that the expression of OATP diminishes during hepatocarcinogenesis[26]. Moreover, OATP 8 expression level decreases prior to complete neoangiogenesis, with elevation of arterial flow and reduction of portal venous flow[27]. Thanks to their lipophilic characteristics, HCAs, after the intravascular/interstitial distribution, are taken up by functioning hepatocytes, metabolized, and excreted into the bile through the OATP 8: Consequently, nodules with low or no OATP expression (the majority of HCC, many early HCCs, and some high-grade dysplastic nodules) do not uptake HCAs and appear hypointense in the hepatobiliary phase (HBP) (Figure 2). A recent meta-analysis has shown that the impact of HBP on a per-lesion sensitivity is significant, in particular the use of Gd-EOB-DTPA allowed a sensitivity of 87% *vs* 74% ($P = 0.03$) the one without HBP[28]. Based on these considerations, the current contrast agents applied in the study of the liver are the gadobenate dimeglumine (Gd-BOPTA/Dimeg, MultiHance®, Bracco, Milan, Italy), which is a chelate of the paramagnetic gadolinium ion salified with two molecules of meglumine, and gadolinium ethoxybenzyl diethylenetriaminepentaacetic acid (Gd-EOB-DTPA, Primovist®, Bayer Schering Pharma, Berlin, Germany), which is a highly water-soluble contrast agent with an ethobenzyl group attached to gadolinium diethylenetriamine pentaacetic acid[29]. The approved dose of Gd-BOPTA for hepatic imaging is 0.05 mmol/kg (0.1 mL/kg of a 0.5 mol/L solution)[30], and it should be administered undiluted followed by a normal saline "flush" of 20 to 50 mL. Hepatic uptake represents 2%-4% of the injected dose for Gd-BOPTA, and the HBP is typically performed between 45 and 120 min after injection and is necessary in order to achieve sufficient enhancement.

The approved dose of Gd-EOB-DTPA is 0.025 mmol/kg, which is considered the minimum effective dose for the detection of liver lesions in the hepatobiliary phase.

Lesion	Sequences						
	Unenhanced T1	Arterial	Portal venous	Delayed	Hepatobiliary	DWI	T2
ECA — HCC classic							
ECA — HCC green							
ECA — HCC hypovascular							
HBA — HCC classic							
HBA — HCC green							
HBA — HCC hypovascular							

Isointense lesion   Hyperintense lesion   Hypointense lesion   Slightly hyperintense lesion

Figure 2 Schematic representation showing dynamic contrast enhanced sequences, diffusion weighted images, and T2-weighted features in typical, green, and hypovascular hepatocellular carcinoma, comparing information from extracellular contrast agent and hepatobiliary contrast agent. ECA: Extracellular contrast agent; HBA: Hepatobiliary contrast agent; DWI: Diffusion weighted images.

The modalities of gadoxetic acid administration were addressed in the ESGAR consensus statement[31] (flow-rate of 1-2 mL/s followed by a 20 mL saline flush at 1-2 mL/s using a bolus triggering technique). Hepatic uptake represents 50% for Gd-EOB-DTPA, and the HBP reaches its maximum intensity approximately 20 min after injection with gadoxetate disodium and persists for several hours[32]. The clinical use of liver-specific contrast agents allows the radiologist to obtain morphologic and vascular-related information, although an overlap between delayed phase and hepatocyte phase have to be considered during dynamic evaluation[33]. A recent meta-analysis[34] reported that in trials of MRI that directly compared test performance using different contrast agents, use of HCAs was associated with higher sensitivity than ECAs (difference of 13%), with no difference in specificity. The difference was somewhat greater for HCC lesions smaller than 2 cm (difference of 15%). These finding were stressed by the ESGAR consensus[31], who stated that a Gd-EOB-DTPA MR examination should be performed in order to characterize an undetermined focal liver lesion of 10 mm or larger in the cirrhotic liver. In summary, HCAs allow a comprehensive non-invasive imaging assessment of the liver parenchyma, intrahepatic lesions depiction or characterization, hepatic vasculature, and the biliary tree in a single examination. They have several advantages in the evaluation of the cirrhotic liver including: (1) Higher sensitivity for the diagnosis of HCC, in particular for lesions smaller than 2 cm[34]; (2) improved characterization of arterially enhancing lesions without definite washout on subsequent imaging[35]; (3) the possibility to differentiate arterially enhancing lesion *vs* pseudolesions[36]; and (4) detection of lesions with decreased uptake evidenced only in the HBP that are likely to be precancerous or borderline lesion[37].

PERFUSION IMAGING

Perfusion MRI in the assessment of HCC focuses on the detection and characterization of lesions[38-40], the evaluation of response to therapy[38,41-44], and determination of prognosis[44,45] (Table 2).

The basis of dynamic contrast-enhanced (DCE)-perfusion MR imaging is the acquisition of multiple image sets, every few seconds, through the tumor or as much of the organ as possible, after gadolinium injection. The rate and pattern of contrast enhancement reflects

Table 2 Magnetic resonance imaging perfusion with dynamic contrast-enhanced magnetic resonance imaging in the assessment of hepatocellular carcinoma, focus on diagnosis, characterization, response to therapy, and prognosis

Ref.	Year	Magnet (Tesla)	Contrast agent	Parameters
Diagnosis and characterization				
Taouli *et al*[38]	2013	1.5 T	Gadobenate-dimeglumine and gadopentetate-dimeglumine	AF, VF, ART, DV, MTT
Chen *et al*[39]	2017	3 T	GD-EOB-DTPA	Ktrans, Kep, iAUC, max-Ktrans
Jajamovich *et al*[40]	2016	3 T	Gadobenate-dimeglumine	ART, K trans, ve, kep, τ
Abdullah *et al*[61]	2008	1.5 T	Gadoterate-dimeglumine	HPI, MTT, DV, TF, AF, PF
Response to therapy				
Ippolito *et al*[41]	2016	1.5 T	GD-EOB-DTPA	ME, MRE, RAE, RE, RLE, RVE, TTP
Taouli *et al*[38]	2013	1.5 T	Gadobenate-dimeglumine and Gadopentetate-dimeglumine	AF, VF, ART, DV, MTT
Chen *et al*[45]	2016	1.5 T	Gadodiamide	Peak, Slope, AUC, Ktrans, Kep, Ve
Prognosis				
Chen *et al*[45]	2016	1.5 T	Gadodiamide	Peak, Slope, AUC, Ktrans, Kep, Ve
Chen *et al*[45]	2016	1.5 T	Gadodiamide	ART, AF, PF, TF, MTT, DV, PEAK, SLOPE, AUC

ART: Arterial fraction; K trans: Contrast agent transfer rate constant from plasma to extravascular extracellular space; VE: Extravascular extracellular volume fraction; Kep: Contrast agent intravasation rate constant; τ: Mean intracellular water molecule lifetime; ME: Maximum enhancement; MRE: Maximum relative enhancement; RAE: Relative arterial enhancement; RE: Relative enhancement; RLE: Relative late enhancement; RVE: Relative venous enhancement; TTP: Time to peak; HPI: Hepatic perfusion index; MTT: Mean transit time; DV: Distribution volume; TF: Total blood flow; AF: Arterial blood flow; PF: Portal blood flow; AUC: Area under the gadolinium distribution-time curve.

the time evolution of the contrast agent within the tissue, which occurs as a result of the microcirculatory pathophysiological changes. Perfusion MRI could extend the currently used qualitative assessment applied for the differential diagnosis of lesions, by applying quantitative metrics to describe their vascular behaviour.

The main purpose of MRI perfusion is the quantification of vascular characteristics of HCC, because the growth and progression of histological malignancy of HCC are associated with new blood vessels formation[46] (angiogenesis). Moreover, the targets of anti-angiogenic drugs, recently used for HCC treatment, are represented by these new blood vessels and, therefore, the perfusion, as a functional imaging technique, may be suitable for evaluating patients treated with these agents[47-50].

Dynamic contrast-enhanced magnetic resonance imaging (DCE-MRI) provides non-invasive imaging biomarkers that can measure changes in tumor blood flow, vascular permeability, and interstitial and intravascular volumes[40,43,47] and can predict the survival outcome in patients with HCC[51-53]. Generally, DCE-MRI consists of acquisition of T1-weighted MR images before, during, and after intravenous injection of a gadolinium-based contrast agent[40]. The contrast agent extravasates at level of tumor tissue, from intravascular to the extravascular extracellular space (EES) with increased T1-w signal[43,54,55]. This extravasation to EES in the tumor tissue depends on vessel leakiness (permeability) and blood flow (perfusion), and so the signal measured with DCE-MRI could be sensitive to alterations in vascular permeability, EES, and blood flow[43,54].

DCE-MRI signals can be quantified using a semi-quantitative (model free) or quantitative (model based) analysis[56]. Both analysis methods have several parameters related with tumor angiogenesis[54,57] and can give different information on liver and tumor perfusion[56].

Briefly, with the semi-quantitative analysis, all perfusion parameters are extracted directly from time-signal intensity (SI) curves [*e.g.*, AUC, maximum SI or peak enhancement ratio, wash-in slope, mean transit time (MTT)], derived from different dynamic contrastographic sequences. Although widely used, semi-quantitative analysis is highly affected by the acquisition systems and comparison and quantification of these parameters can be difficult[56,57] because the true concentration of contrast agent in the tissues is not estimated (Figure 3).

Quantitative analysis depends on fitting the time SI curves with the changes in concentration of the contrast agent using pharmacokinetic techniques using several kinetics models based on different physiological assumptions made[56]. These kinetics models can be bi-compartmental models (taking into account vessels and EES) or mono-compartmental (taking into account the vascular space because of the typical architecture of the liver)[56], with a double or single input system (arterial and portal or arterial alone), conventional compartment (CC) models vs distributed parameters (DP) models[54,56].

Several parameters extracted with quantitative analysis are related to the influx of contrast agent from the intravascular space to the EES (K trans) and its reverse (Kep), the volume fraction of EES (Ve), which is an indirect expression of the cellular density of the tissue[43,54,56].

In comparison to the semi-quantitative analysis, these parameters are more time consuming because they generate parametric maps through a pixel-by-pixel curve fitting process. Although the histogram analysis and the heterogeneity of these parametric maps are more computationally demanding, they may also provide additional information[43,56]. Moreover, numerous pharmacokinetic models have been proposed by Tofts
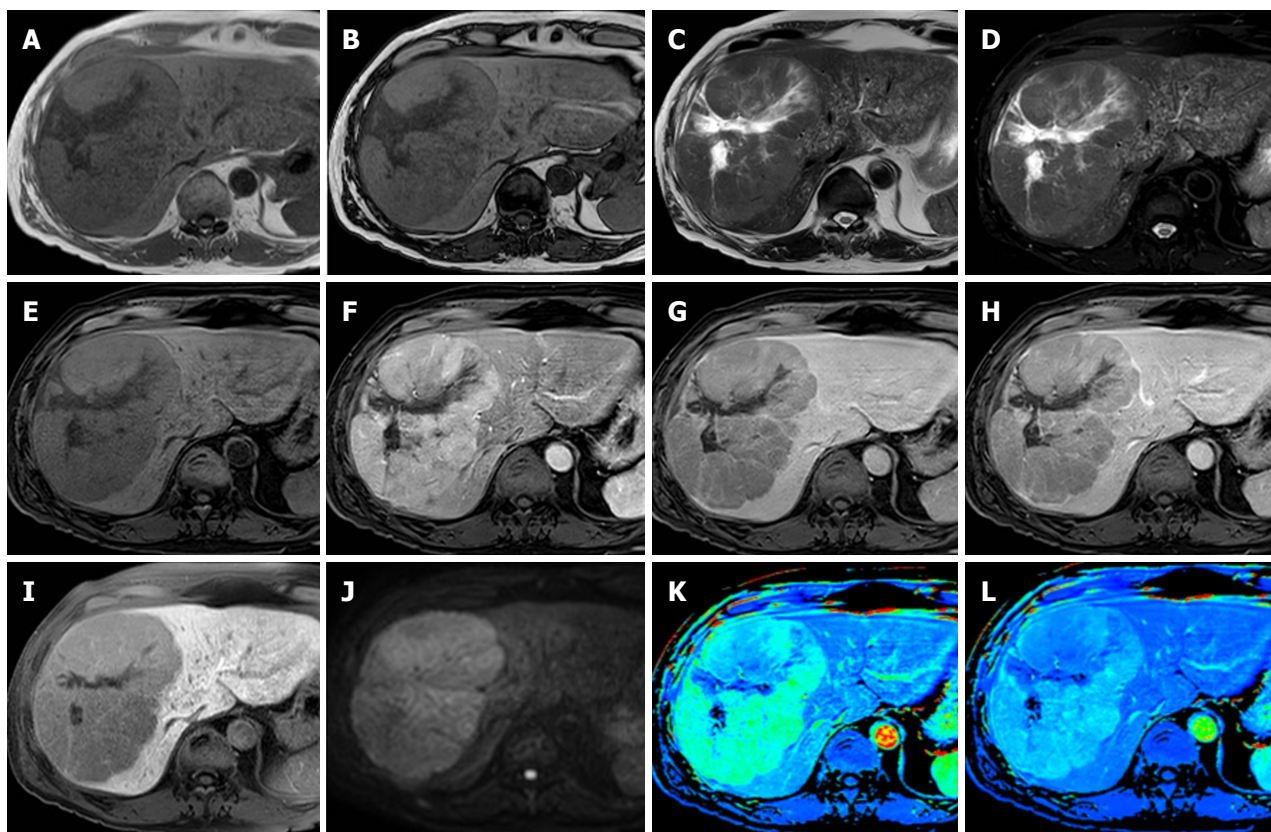
Figure 3 Gd-EOB-DTPA enhanced magnetic resonance images of a 67-year-old male patient with large hepatocellular carcinoma lesion in the right liver lobe. Panels A-B: T1-weighted sequences "in and out of phase" demonstrate a heterogeneous mass slightly hypointense without a signal drop in "out of phase" sequence. Panels C-D: T2-weighted image without and with fat saturation demonstrates a slightly hyperintense mass with a central, homogeneous hyperintense area, as per necrosis. Panels E-H: Dynamic contrast-enhanced images delineate the typical contrast behavior of hepatocellular carcinoma (HCC): Hyperenhancement during the arterial phase (F) followed by wash-out in portal and delayed phase (G-H). In the hepatobiliary phase image 20 min after Gd-EOB-DTPA injection the nodule appears highly hypointense compared with the surrounding enhanced liver (panel I). Panel J: On the diffusion weighted image, HCC lesion is hyperintense due to the restriction of water diffusion. Panel K-L: Perfusion images derived from semiquantitative analysis (relative arterial enhancement and maximum enhancement) the HCC is characterized by high vascularity intensity signals, shown as hot-spots signals.

et al[58], Brix *et al*[59], and Larsson *et al*[60], using a single arterial input function[43]. Because HCC receives major blood supply from hepatic neo-arteries and often arise from a cirrhotic liver, the single input model (considering only the arterial input) and the dual compartment model (because of the alteration in the EES) are frequently both used in the literature[54,56].

However, because of numerous DCE-MRI–related limitations, parameters derived from these pharmacokinetic models may lack sufficient precision for clinical application[38], and there is no consensus regarding the pharmacokinetic model that should be used to quantify HCC perfusion parameters, even if some studies demonstrated that some pharmacokinetic models can be equivalent in the results[40].

All these possibilities and differences in the field of DCE-MRI led to literature studies with different results.

In general, two recent studies demonstrated that HCC had significantly higher peak, slope, AUC, arterial fraction, and arterial flow but lower portal flow, distribution volume, and MTT than the liver[45]. HCCs with high peak are correlated to a longer overall survival (OS) in comparison with HCC with low peak[45]

before systemic therapy. Secondly, high peak reduction assessed early (1 wk) after systemic therapy can be related to OS[44].

DCE-MRI semi-quantitative parameters (relative arterial, venous, and late enhancement; maximum enhancement; maximum relative enhancement, and time to peak) potentially can be used also to differentiate residual viable tumor tissue and effective treated lesions after TACE or RFA[41]. Some of them, in a multivariate analysis, seemed also to predict the response to radiotherapy RT[42].

Some groups found that with DCE-MRI it is possible to quantify the perfusion in the liver and HCC with an increased arterial flow and decreased portal venous flow in HCC compared with cirrhotic liver, with significant differences in the degree of arterial versus portal venous blood flow in treated and untreated HCCs[38].

Perfusion parameters could be correlated to the grading differentiation of HCC, but in most of the cases, there were no significant differences in perfusions and grade of HCC differentiation, with the exception of the arterial fraction (ART)[40]. The ART parameter is a value estimated each time through perfusion equations

obtained from the addition of the two input inflow (arterial and portal) into one[40]. Moreover, it has been suggested that ART can be used to assess response to local regional therapy in HCC[38,40,61].

In a recent study from Chen *et al*[39], the max-Ktrans seemed to correlate with tumor grades (rho = -0.382, *P* = 0.028). The Ktrans, Kep, and iAUC of high-grades HCC were significantly lower than that of low-grades HCC (*P* = 0.001, 0.031, 0.003, respectively), but there was no statistically significant differences for Ve between high grade and low grade HCC (*P* > 0.05)[39].

These results suggest that DCE-MRI can be useful as a non-invasive marker of HCC angiogenesis, but new equipment and sequences and models are still under investigation. New equipment will be applied in the near future to quantify the perfusion of HCC, as a biomarker of degree of malignancy, prognosis, and response to therapy[38-40].

DIFFUSION WEIGHTED IMAGING

DWI is a functional MRI sequence that allow the characterization of biological tissues based on the diffusion properties of water molecules, providing information about tissue cellularity and about the integrity of cellular membranes[2]. In fact, in high cellular tissue, the higher density of hydrophobic cellular membranes reduces the "apparent" diffusion of water protons[62], thus the water diffusion can be considered relatively "restricted". More simply the "diffusion restriction" refers to a tumor signal intensity that is higher than the surrounding parenchyma (the liver for example) on high b-value DW MR images, and, to date, DW-imaging represents an integral part of the routine MR protocol for liver disease (Figure 4).

In 2010, Taouli *et al*[63] defined DW MR imaging, an attractive technique, which was reaching a potential for clinical use in the abdomen, particularly in the liver. Less than a decade later, all the potential uses of DWI are greatly shown, and diffusion can be considered a useful tool for the diagnosis of focal liver lesions, with better results than T2-weighted images[64] especially in HCC[65]. There are various reasons why: DWI adds useful qualitative and quantitative information to standard sequences; it has a short acquisition time and can be easily included to existing protocols; and it does not need the use of contrast materials[66,67].

Although several DW imaging sequences can be applied to evaluate the liver, the single shot spin-echo (SE) echo-planar technique is the most frequently used in combination with fat suppression. Recent studies[68] compared free breathing (FB) *vs* respiratory triggered (RT) DWI for detecting HCC, using a 3 T scanner, a 32-channel torso-cardiac phased-array coil, and dual-source parallel radiofrequency excitation and transmission technology. They concluded that FB-DWI provided better image quality and showed higher detectability of HCCs in patients with chronic liver disease compared to RT-DWI, without significantly

reducing the SNR of the normal liver parenchyma or the lesion-to-non lesion CNR. DW imaging should not be considered a stand-alone sequence, but should be integrated in MR protocols: The combination of Gd-EOB-DTPA and DWI could allow the assessment of the three main processes in the hepatic multistep carcinogenesis (vascular changes, hepatocyte change, and tissue diffusivity). A recent meta-analysis showed that the combination of gadoxetic acid-enhanced MRI and DWI significantly improved both diagnostic accuracy and specificity for HCCs associated with chronic liver disease[69]. Several studies underline the importance that DWI adds to dynamic contrast-enhanced MRI, in characterization of small or atypically enhancing lesions[70,71]. In particular, Briani *et al*[71] demonstrated that the hypovascular lesions ≥ 10 mm that appeared hyperintense in DWI are associated with progression to hypervascular HCC. DWI can not only indicate the morphological characteristics of a lesion with a qualitative assessment, but with apparent diffusion coefficient (ADC) measurement, can also provide a quantitative index of diffusion characteristics, analyzing structure and tissue components. Some authors[70,72] suggested that a lesion-to-liver ADC ratio cut-off value of 0.92 may offer good sensitivity, specificity, and accuracy in differentiating HCC *vs* dysplastic nodules (DN). Inchingolo *et al*[70], furthermore, obtained higher values (sensitivity 90.91%, specificity 80.95%, and accuracy of 83.55%, when the group of LGDNs was compared to the group that included both HGDNs and HCCs, with a cut-off of 0.95. Jiang *et al*[73] conducted a retrospective analysis of the correlation between qualitative and quantitative DWI and HCC tumor grade. They found that while SI values on DWI could distinguish only between well-differentiated HCC and moderately or poorly differentiated HCC, ADC values could distinguish between well, moderately, and poorly differentiated HCC, with the consequence of a better pre-operative and non-invasive histological characterization. Further applications of DW imaging are still ongoing, and larger studies are needed to validate these results. One example is the application of DWI concerning the prediction of microvascular invasion (MVI) in HCC. MVI still remains one of the important prognostic factors of HCC recurrence, especially after surgical resection or liver transplantation[74,75]. In the past, other imaging characteristics have previously been suggested as predictors of MVI, such as tumor size, shape and margin, capsule, peritumoral enhancement, and dynamic enhancement pattern; but recently Yang *et al*[76] proposed a new integrated evaluation of T2 and DWI images by defining the concept of "diffusion- and T2-weighted imaging mismatch". They demonstrated that this new "DWI/T2 mismatch" was an independent predictor of MVI (odds ratio 4.521, *P* = 0.035), with a high specificity (95.65%). Another potential application of DWI is the assessment of liver tumor response to novel therapy. In fact, while a change in tumor size is
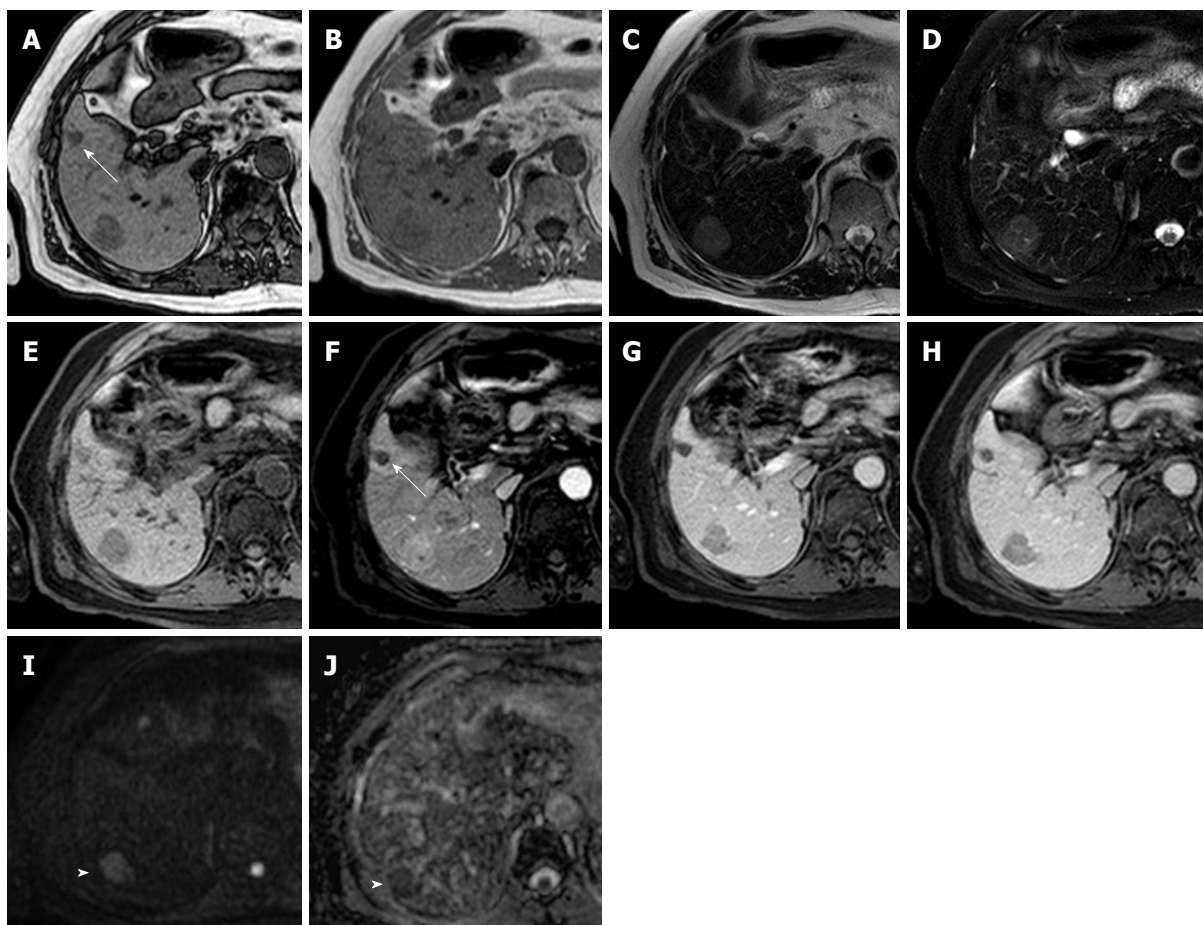
Figure 4 Gd-EOB-DTPA enhanced magnetic resonance images of a 61-year-old patient with hepatocellular carcinoma nodule in the VII segment of the liver. Panels A-B: A single nodule slightly hypointense on the T1-weighted "in phase" sequence (A) with a signal drop in the "out of phase" sequence, as per fat deposition. Panels C-D: On T2-weighted image without and with fat saturation the nodule appears slightly hyperintense. Panels E-H: Dynamic contrast-enhanced images demonstrate the typical contrast behavior of hepatocellular carcinoma: Which appear hypervascular during the arterial phase (F) with wash-out in portal and delayed phase (G-H). Panel I-J: Diffusion weighted image (DWI) shows the hyperintense pattern of the lesion which appear hypointense on the relative apparent diffusion coefficient map (arrowhead). Previously treated lesion with transarterial chemoembolization is recognizable, in panel A-E-F-G-H, at V segment of the liver (arrow). No any restriction of signal intensity is evident on DWI (panel I-J).

the common effect of conventional chemotherapy, loco-regional therapies may lead to stability of tumor size or even an increase in hepatic tumo. Moreover, novel molecular-targeted therapies may alter the morphology of the tumor by affecting its angiogenesis, with unchanged tumor size[77]. Recent studies have shown the possibility to differentiate viable tissue from necrosis on the basis of ADC cut-off values, because necrosis has higher ADC values[78,79]. For patients with HCC treated with Sorafenib, a transient decrease in tumor ADC value approximately 1 month after treatment has been reported to be suggestive of hemorrhagic necrosis; however, a sustained decrease in ADC at 3-mo follow-up may indicate viable tumor or its progression[80]. ADC values in patients with HCC treated with transarterial radioembolization (TARE) have been shown to increase, a finding suggestive of cellular necrosis. Increased ADC values in such cases may be an early marker of treatment response before changes in tumor size are observed[81]. Despite the several attempts to use ADC values in clinical practice, reproducibility of volumetric

quantification with diffusion-weighted imaging is not well established. Moreover, there are some technical aspects that need to be considered, like the differences in scanner equipments, the lack of a standardized DWI protocol, the low reproducibility and comparability of ADC measurements among different studies, and finally, the susceptibility of ADC maps to noise and artefacts[64].

MR ELASTOGRAPHY

MR elastography (MRE) is an MRI-based method for the quantitative assessment of liver fibrosis and increased stiffness. This technique is based on the application of mechanical waves (generated through the machine) to the region of interest (the liver). These waves and their wave-length are located in the liver through different elastographic sequences (the most used are gradient-echo sequences with motion-encoding gradients) to obtain different set of images and maps. With two different reconstruction algorithms applied to this set of images, it is possible to obtain a final colored image,

called "confidence map", with different stiffness areas of the liver expressed with different colors that correspond to different in kilo-pascal values (kPa).

Different studies have demonstrated the possibility to use MRE for assessment of mild degree of liver fibrosis[82-84] and to differentiate malignant and benign nodules in the liver[85]. A recent study tried to understand if there was a correlation between HCC stiffness detected with MRE and HCC pathologic features[84]. Tumor stiffness (TS) seemed to be higher in moderate/well differentiated HCC in comparison to poor differentiated HCC (6.5 ± 1.2 kPa *vs* 4.9 ± 1.2 kPa, $P < 0.01$); but at the moment, no correlation is found to liver parenchyma stiffness, vascular invasion, and tumor encapsulation[84].

Another important application of MRE regards the assessment to treatment response and in particular loco-regional treatment [[90]Yttrium radio-embolization (RE), trans-arterial chemoembolization (TACE), and radiofrequency ablation (RFA)][86].

In two animal studies[87,88], reduction in TS was associated with histologically proven central necrosis[89] and decreased cellular proliferation and moderate induction of apoptosis[88]. In a preliminary study on humans, MRE seems to provide early evidence of therapeutic response, demonstrating that treated tumors have significantly lower TS compared to untreated tumors (3.9 ± 1.8 kPa *vs* 6.9 ± 3.4 kPa, $P = 0.006$) and cirrhotic liver, while intra-tumoral hemorrhage is associated with higher TS. TS seems to relate with visually assessed percentage of necrosis and ER and is more in patients treated with RE[86].

MRE still has the limitation of hepatic iron overload, which can decrease hepatic signal intensity in gradient echo based MRE sequences to unacceptably low levels[83]. On the other hand, MRE enables qualitative and quantitative assessment of TF without the use of gadolinium chelates[86].

Despite some of the limitations of MRE, it remains a promising technique not only for the evaluation of liver fibrosis but also in the spectrum of diagnosis and prognosis of HCC[83,84,86].

RADIOMICS

Radiomics represents the possibility to convert digital medical images (CT, MR, or positron emission tomography images) into high-dimensional data[89]; the hypothesis is that biomedical images contain information that reflects underlying pathophysiology and that these relationships can be revealed *via* quantitative image analyses. MRI based radiomics signature are currently investigated in glioblastoma, breast, and faringeal cancer. Currently, there are no studies about the possibility to use radiomics in the assessment of HCC. Main efforts remain focused on some complex texture analysis, taking in account just few features, which represent a small and impaired part of radiomics data analysis.

Controversial results were obtained from different studies concerning the use of texture analysis in the assessment of HCC[90-93]. The main problems are due to differences in the equipment, contrast phase chosen for the analysis, and type of segmentation (circular ROI *vs* tumor shape ROI, slice analysis vs volumetric ROI analysis). Recently, two studies have been published on the possibility to use complex texture analysis in MRI to assess the malignancy of HCC (Zhou *et al*[94]) or to predict the progression of hypovascular nodules (detected with gadoxetate disodium acid during hepatobiliary phase) into hypervascular HCC lesions[90]. In both studies, volumetric region of interest (VOI) was evaluated.

All these preliminary studies demonstrated that, among the different features assessed with texture analysis, some of them seem to perform better on a specific dynamic phase (arterial or hepatobiliary) and can give useful information. In order to differentiate low grade and high grade HCC[94], "mean intensity value" (a histogram feature) presented significantly larger values in low-grade HCCs than in the high-grade HCCs, and the values of gray-level run-length nonuniformity (GLN) were significantly smaller in low-grade HCCs than in high-grade HCCs.

Moreover, in another study, different histogram metrics showed the possibility to predict the progression of a hypovascular nodule into an HCC[90], using different flip angles and volumetric region of interest.

Radiomics appears to offer a nearly limitless supply of imaging biomarkers that could potentially aid in cancer detection, diagnosis, assessment of prognosis, prediction of response to treatment, and monitoring of disease status[89]. Further studies and validations are required for the performance of the features by themselves, their application according to the different contrast phases available during MRI sequences, and the different MRI equipment.

CONCLUSION

MRI of the liver represents an important tool for the detection and characterization of focal liver lesions and for the evaluation of diffuse liver disease. The main advantages of MRI relies on superior soft tissue contrast, absence of ionizing radiation, and the possibility of performing functional and advanced imaging techniques. Unlike conventional MR imaging sequences, which are usually reported qualitatively based on the varying brightness of tissue, functional MR-imaging techniques offers quantitative data. Among the different functional MR imaging techniques, DWI, MR elastography, and T1-weighted DCE sequences are the most likely to find clinical use at present or in the near future in liver imaging.

MR functional imaging allows for the addition of qualitative and quantitative functional information to conventional anatomic sequences and routine clinical protocols, thereby offering clinicians further comprehensive

information about the biology, behavior, and prognosis about HCC lesions.

ACKNOWLEDGMENTS

REFERENCES

1   **Ferlay J**, Soerjomataram I, Dikshit R, Eser S, Mathers C, Rebelo M, Parkin DM, Forman D, Bray F. Cancer incidence and mortality worldwide: sources, methods and major patterns in GLOBOCAN 2012. *Int J Cancer* 2015; **136**: E359-E386 [PMID: 25220842 DOI: 10.1002/ijc.29210]

2   **El-Serag HB**, Mason AC. Rising incidence of hepatocellular carcinoma in the United States. *N Engl J Med* 1999; **340**: 745-750 [PMID: 10072408 DOI: 10.1056/NEJM199903113401001]

3   **Sangiovanni A**, Prati GM, Fasani P, Ronchi G, Romeo R, Manini M, Del Ninno E, Morabito A, Colombo M. The natural history of compensated cirrhosis due to hepatitis C virus: A 17-year cohort study of 214 patients. *Hepatology* 2006; **43**: 1303-1310 [PMID: 16729298 DOI: 10.1002/hep.21176]

4   **Bosch FX**, Ribes J, Cléries R, Díaz M. Epidemiology of hepatocellular carcinoma. *Clin Liver Dis* 2005; **9**: 191-211, v [PMID: 15831268 DOI: 10.1016/j.cld.2004.12.009]

5   **Singal AK**, Singh A, Jaganmohan S, Guturu P, Mummadi R, Kuo YF, Sood GK. Antiviral therapy reduces risk of hepatocellular carcinoma in patients with hepatitis C virus-related cirrhosis. *Clin Gastroenterol Hepatol* 2010; **8**: 192-199 [PMID: 19879972 DOI: 10.1016/j.cgh.2009.10.026]

6   **Zanetti AR**, Van Damme P, Shouval D. The global impact of vaccination against hepatitis B: a historical overview. *Vaccine* 2008; **26**: 6266-6273 [PMID: 18848855 DOI: 10.1016/j.vaccine.2008.09.056]

7   **Mittal S**, El-Serag HB. Epidemiology of hepatocellular carcinoma: consider the population. *J Clin Gastroenterol* 2013; **47** Suppl: S2-S6 [PMID: 23632345 DOI: 10.1097/MCG.0b013e3182872f29. Epidemiology]

8   **Dyson J**, Jaques B, Chattopadyhay D, Lochan R, Graham J, Das D, Aslam T, Patanwala I, Gaggar S, Cole M, Sumpter K, Stewart S, Rose J, Hudson M, Manas D, Reeves HL. Hepatocellular cancer: the impact of obesity, type 2 diabetes and a multidisciplinary team. *J Hepatol* 2014; **60**: 110-117 [PMID: 23978719 DOI: 10.1016/j.jhep.2013.08.011]

9   **Siegel AB**, Zhu AX. Metabolic syndrome and hepatocellular carcinoma: two growing epidemics with a potential link. *Cancer* 2009; **115**: 5651-5661 [PMID: 19834957 DOI: 10.1002/cncr.24687]

10   **Kudo M**. Multistep human hepatocarcinogenesis: correlation of imaging with pathology. *J Gastroenterol* 2009; **44** Suppl 19: 112-118 [PMID: 19148804 DOI: 10.1007/s00535-008-2274-6]

11   **European Association For The Study Of The Liver**; European Organisation For Research And Treatment Of Cancer. EASL-EORTC clinical practice guidelines: management of hepatocellular carcinoma. *J Hepatol* 2012; **56**: 908-943 [PMID: 22424438 DOI: 10.1016/j.jhep.2011.12.001]

12   **Bruix J**, Sherman M; American Association for the Study of Liver Diseases. Management of hepatocellular carcinoma: an update. *Hepatology* 2011; **53**: 1020-1022 [PMID: 21374666 DOI: 10.1002/hep.24199]

13   **Colli A**, Fraquelli M, Casazza G, Massironi S, Colucci A, Conte D, Duca P. Accuracy of ultrasonography, spiral CT, magnetic resonance, and alpha-fetoprotein in diagnosing hepatocellular carcinoma: a systematic review. *Am J Gastroenterol* 2006; **101**: 513-523 [PMID: 16542288 DOI: 10.1111/j.1572-0241.2006.00467.x]

14   **Burrel M**, Llovet JM, Ayuso C, Iglesias C, Sala M, Miquel R, Caralt T, Ayuso JR, Solé M, Sanchez M, Brú C, Bruix J; Barcelona Clínic Liver Cancer Group. MRI angiography is superior to helical CT for detection of HCC prior to liver transplantation: an explant correlation. *Hepatology* 2003; **38**: 1034-1042 [PMID: 14512891 DOI: 10.1053/jhep.2003.50409]

15   **Kim BR**, Lee JM, Lee DH, Yoon JH, Hur BY, Suh KS, Yi NJ, Lee KB, Han JK. Diagnostic Performance of Gadoxetic Acid-enhanced Liver MR Imaging versus Multidetector CT in the Detection of Dysplastic Nodules and Early Hepatocellular Carcinoma. *Radiology* 2017; **285**: 134-146 [PMID: 28609205 DOI: 10.1148/radiol.2017162080]

16   **Golfieri R**, Garzillo G, Ascanio S, Renzulli M. Focal lesions in the cirrhotic liver: their pivotal role in gadoxetic acid-enhanced MRI and recognition by the Western guidelines. *Dig Dis* 2014; **32**: 696-704 [PMID: 25376286 DOI: 10.1159/000368002]

17   **Park MJ**, Kim YK, Lee MW, Lee WJ, Kim YS, Kim SH, Choi D, Rhim H. Small hepatocellular carcinomas: improved sensitivity by combining gadoxetic acid-enhanced and diffusion-weighted MR imaging patterns. *Radiology* 2012; **264**: 761-770 [PMID: 22843769 DOI: 10.1148/radiol.12112517]

18   **Xiao YD**, Paudel R, Liu J, Ma C, Zhang ZS, Zhou SK. MRI contrast agents: Classification and application (Review). *Int J Mol Med* 2016; **38**: 1319-1326 [PMID: 27666161 DOI: 10.3892/ijmm.2016.2744]

19   **Balci NC**, Semelka RC. Contrast agents for MR imaging of the liver. *Radiol Clin North Am* 2005; **43**: 887-898, viii [PMID: 16098345 DOI: 10.1016/j.rcl.2005.05.004]

20   **Bellin MF**. MR contrast agents, the old and the new. *Eur J Radiol* 2006; **60**: 314-323 [PMID: 17005349 DOI: 10.1016/j.ejrad.2006.06.021]

21   **Verloh N**, Utpatel K, Haimerl M, Zeman F, Fellner C, Fichtner-Feigl S, Teufel A, Stroszczynski C, Evert M, Wiggermann P. Liver fibrosis and Gd-EOB-DTPA-enhanced MRI: A histopathologic correlation. *Sci Rep* 2015; **5**: 15408 [PMID: 26478097 DOI: 10.1038/srep15408]

22   **Park HJ**, Choi BI, Lee ES, Park SB, Lee JB. How to Differentiate Borderline Hepatic Nodules in Hepatocarcinogenesis: Emphasis on Imaging Diagnosis. *Liver Cancer* 2017; **6**: 189-203 [PMID: 28626731 DOI: 10.1159/000455949]

23   **Marrero JA**, Hussain HK, Nghiem HV, Umar R, Fontana RJ, Lok AS. Improving the prediction of hepatocellular carcinoma in cirrhotic patients with an arterially-enhancing liver mass. *Liver Transpl* 2005; **11**: 281-289 [PMID: 15719410 DOI: 10.1002/lt.20357]

24   **Khalili K**, Kim TK, Jang HJ, Haider MA, Khan L, Guindi M, Sherman M. Optimization of imaging diagnosis of 1-2 cm hepatocellular carcinoma: an analysis of diagnostic performance and resource utilization. *J Hepatol* 2011; **54**: 723-728 [PMID: 21156219 DOI: 10.1016/j.jhep.2010.07.025]

25   **Golfieri R**, Renzulli M, Lucidi V, Corcioni B, Trevisani F, Bolondi L. Contribution of the hepatobiliary phase of Gd-EOB-DTPA-enhanced MRI to Dynamic MRI in the detection of hypovascular small (≤ 2 cm) HCC in cirrhosis. *Eur Radiol* 2011; **21**: 1233-1242 [PMID: 21293864 DOI: 10.1007/s00330-010-2030-1]

26   **Kitao A**, Matsui O, Yoneda N, Kozaka K, Shinmura R, Koda W, Kobayashi S, Gabata T, Zen Y, Yamashita T, Kaneko S, Nakanuma Y. The uptake transporter OATP8 expression decreases during multistep hepatocarcinogenesis: correlation with gadoxetic acid enhanced MR imaging. *Eur Radiol* 2011; **21**: 2056-2066 [PMID: 21626360 DOI: 10.1007/s00330-011-2165-8]

27   **Tsuboyama T**, Onishi H, Kim T, Akita H, Hori M, Tatsumi M, Nakamoto A, Nagano H, Matsuura N, Wakasa K, Tomoda K. Hepatocellular carcinoma: hepatocyte-selective enhancement at gadoxetic acid-enhanced MR imaging--correlation with expression of sinusoidal and canalicular transporters and bile accumulation. *Radiology* 2010; **255**: 824-833 [PMID: 20501720 DOI: 10.1148/radiol.10091557]

28   **Lee YJ**, Lee JM, Lee JS, Lee HY, Park BH, Kim YH, Han JK, Choi BI. Hepatocellular carcinoma: diagnostic performance of multidetector CT and MR imaging-a systematic review and meta-

analysis. *Radiology* 2015; **275**: 97-109 [PMID: 25559230 DOI: 10.1148/radiol.14140690]

29   **Lee NK**, Kim S, Lee JW, Lee SH, Kang DH, Kim GH, Seo HI. Biliary MR imaging with Gd-EOB-DTPA and its clinical applications. *Radiographics* 2009; **29**: 1707-1724 [PMID: 19959517 DOI: 10.1148/rg.296095501]

30   **Schneider G**, Maas R, Schultze Kool L, Rummeny E, Gehl HB, Lodemann KP, Kirchin MA. Low-dose gadobenate dimeglumine versus standard dose gadopentetate dimeglumine for contrast-enhanced magnetic resonance imaging of the liver: an intra-individual crossover comparison. *Invest Radiol* 2003; **38**: 85-94 [PMID: 12544071 DOI: 10.1097/01.RLI.0000044931.26224.F9]

31   **Neri E**, Bali MA, Ba-Ssalamah A, Boraschi P, Brancatelli G, Alves FC, Grazioli L, Helmberger T, Lee JM, Manfredi R, Martì-Bonmatì L, Matos C, Merkle EM, Op De Beeck B, Schima W, Skehan S, Vilgrain V, Zech C, Bartolozzi C. ESGAR consensus statement on liver MR imaging and clinical use of liver-specific contrast agents. *Eur Radiol* 2016; **26**: 921-931 [PMID: 26194455 DOI: 10.1007/s00330-015-3900-3]

32   **Hamm B**, Staks T, Mühler A, Bollow M, Taupitz M, Frenzel T, Wolf KJ, Weinmann HJ, Lange L. Phase I clinical evaluation of Gd-EOB-DTPA as a hepatobiliary MR contrast agent: safety, pharmacokinetics, and MR imaging. *Radiology* 1995; **195**: 785-792 [PMID: 7754011 DOI: 10.1148/radiology.195.3.7754011]

33   **Nakamura Y**, Toyota N, Date S, Oda S, Namimoto T, Yamashita Y, Beppu T, Awai K. Clinical significance of the transitional phase at gadoxetate disodium-enhanced hepatic MRI for the diagnosis of hepatocellular carcinoma: preliminary results. *J Comput Assist Tomogr* 2011; **35**: 723-727 [PMID: 22082543 DOI: 10.1097/RCT.0b013e3182372c40]

34   **Chou R**, Cuevas C, Fu R, Devine B, Wasson N, Ginsburg A, Zakher B, Pappas M, Graham E, Sullivan SD. Imaging Techniques for the Diagnosis of Hepatocellular Carcinoma: A Systematic Review and Meta-analysis. *Ann Intern Med* 2015; **162**: 697-711 [PMID: 25984845 DOI: 10.7326/M14-2509]

35   **Kudo M**, Matsui O, Izumi N, Iijima H, Kadoya M, Imai Y; Liver Cancer Study Group of Japan. Surveillance and diagnostic algorithm for hepatocellular carcinoma proposed by the Liver Cancer Study Group of Japan: 2014 update. *Oncology* 2014; **87** Suppl 1: 7-21 [PMID: 25427729 DOI: 10.1159/000368141]

36   **Motosugi U**, Ichikawa T, Sou H, Sano K, Tominaga L, Muhi A, Araki T. Distinguishing hypervascular pseudolesions of the liver from hypervascular hepatocellular carcinomas with gadoxetic acid-enhanced MR imaging. *Radiology* 2010; **256**: 151-158 [PMID: 20574092 DOI: 10.1148/radiol.10091885]

37   **Kumada T**, Toyoda H, Tada T, Sone Y, Fujimori M, Ogawa S, Ishikawa T. Evolution of hypointense hepatocellular nodules observed only in the hepatobiliary phase of gadoxetate disodium-enhanced MRI. *AJR Am J Roentgenol* 2011; **197**: 58-63 [PMID: 21701011 DOI: 10.2214/AJR.10.5390]

38   **Taouli B**, Johnson RS, Hajdu CH, Oei MT, Merad M, Yee H, Rusinek H. Hepatocellular carcinoma: perfusion quantification with dynamic contrast-enhanced MRI. *AJR Am J Roentgenol* 2013; **201**: 795-800 [PMID: 24059368 DOI: 10.2214/AJR.12.9798]

39   **Chen J**, Chen C, Xia C, Huang Z, Zuo P, Stemmer A, Song B. Quantitative free-breathing dynamic contrast-enhanced MRI in hepatocellular carcinoma using gadoxetic acid: correlations with Ki67 proliferation status, histological grades, and microvascular density. *Abdom Radiol (NY)* 2018; **43**: 1393-1403 [PMID: 28939963 DOI: 10.1007/s00261-017-1320-3]

40   **Jajamovich GH**, Huang W, Besa C, Li X, Afzal A, Dyvorne HA, Taouli B. DCE-MRI of hepatocellular carcinoma: perfusion quantification with Tofts model versus shutter-speed model--initial experience. *MAGMA* 2016; **29**: 49-58 [PMID: 26646522 DOI: 10.1007/s10334-015-0513-4]

41   **Ippolito D**, Trattenero C, Talei Franzesi C, Casiraghi A, Lombardi S, Vacirca F, Corso R, Sironi S. Dynamic Contrast-Enhanced Magnetic Resonance Imaging With Gadolinium Ethoxybenzyl Diethylenetriamine Pentaacetic Acid for Quantitative Assessment of Vascular Effects on Hepatocellular-Carcinoma Lesions Treated

by Transarterial Chemoembolization or Radiofrequency Ablation. *J Comput Assist Tomogr* 2016; **40**: 692-700 [PMID: 27560010 DOI: 10.1097/RCT.0000000000000427]

42   **Liang PC**, Ch'ang HJ, Hsu C, Chen LT, Shih TT, Liu TW. Perfusion parameters of dynamic contrast-enhanced magnetic resonance imaging predict outcomes of hepatocellular carcinoma receiving radiotherapy with or without thalidomide. *Hepatol Int* 2015; **9**: 258-268 [PMID: 25788178 DOI: 10.1007/s12072-014-9557-1]

43   **Chen BB**, Shih TT. DCE-MRI in hepatocellular carcinoma-clinical and therapeutic image biomarker. *World J Gastroenterol* 2014; **20**: 3125-3134 [PMID: 24695624 DOI: 10.3748/wjg.v20.i12.3125]

44   **Chen BB**, Hsu CY, Yu CW, Liang PC, Hsu C, Hsu CH, Cheng AL, Shih TT. Early perfusion changes within 1 week of systemic treatment measured by dynamic contrast-enhanced MRI may predict survival in patients with advanced hepatocellular carcinoma. *Eur Radiol* 2017; **27**: 3069-3079 [PMID: 27957638 DOI: 10.1007/s00330-016-4670-2]

45   **Chen BB**, Hsu CY, Yu CW, Liang PC, Hsu C, Hsu CH, Cheng AL, Shih TT. Dynamic Contrast-enhanced MR Imaging of Advanced Hepatocellular Carcinoma: Comparison with the Liver Parenchyma and Correlation with the Survival of Patients Receiving Systemic Therapy. *Radiology* 2016; **281**: 454-464 [PMID: 27171020 DOI: 10.1148/radiol.2016152659]

46   **Folkman J**. Is angiogenesis an organizing principle in biology and medicine? *J Pediatr Surg* 2007; **42**: 1-11 [PMID: 17208533 DOI: 10.1016/j.jpedsurg.2006.09.048]

47   **De Robertis R**, Tinazzi Martini P, Demozzi E, Puntel G, Ortolani S, Cingarlini S, Ruzzenente A, Guglielmi A, Tortora G, Bassi C, Pederzoli P, D'Onofrio M. Prognostication and response assessment in liver and pancreatic tumors: The new imaging. *World J Gastroenterol* 2015; **21**: 6794-6808 [PMID: 26078555 DOI: 10.3748/wjg.v21.i22.6794]

48   **Duffy AG**, Ulahannan SV, Cao L, Rahma OE, Makarova-Rusher OV, Kleiner DE, Fioravanti S, Walker M, Carey S, Yu Y, Venkatesan AM, Turkbey B, Choyke P, Trepel J, Bollen KC, Steinberg SM, Figg WD, Greten TF. A phase II study of TRC105 in patients with hepatocellular carcinoma who have progressed on sorafenib. *United European Gastroenterol J* 2015; **3**: 453-461 [PMID: 26535124 DOI: 10.1177/2050640615583587]

49   **O'Connor JP**, Jackson A, Parker GJ, Roberts C, Jayson GC. Dynamic contrast-enhanced MRI in clinical trials of antivascular therapies. *Nat Rev Clin Oncol* 2012; **9**: 167-177 [PMID: 22330689 DOI: 10.1038/nrclinonc.2012.2]

50   **Fischer MA**, Kartalis N, Grigoriadis A, Loizou L, Stål P, Leidner B, Aspelin P, Brismar TB. Perfusion computed tomography for detection of hepatocellular carcinoma in patients with liver cirrhosis. *Eur Radiol* 2015; **25**: 3123-3132 [PMID: 25903707 DOI: 10.1007/s00330-015-3732-1]

51   **Yuan Z**, Li WT, Ye XD, Zhu HY, Peng WJ. Novel functional magnetic resonance imaging biomarkers for assessing response to therapy in hepatocellular carcinoma. *Clin Transl Oncol* 2014; **16**: 599-605 [PMID: 24356932 DOI: 10.1007/s12094-013-1147-5]

52   **Lee SH**, Hayano K, Zhu AX, Sahani DV, Yoshida H. Water-Exchange-Modified Kinetic Parameters from Dynamic Contrast-Enhanced MRI as Prognostic Biomarkers of Survival in Advanced Hepatocellular Carcinoma Treated with Antiangiogenic Monotherapy. *PLoS One* 2015; **10**: e0136725 [PMID: 26366997 DOI: 10.1371/journal.pone.0136725]

53   **Lee SH**, Hayano K, Zhu AX, Sahani DV, Yoshida H. Dynamic Contrast-Enhanced MRI Kinetic Parameters as Prognostic Biomarkers for Prediction of Survival of Patient with Advanced Hepatocellular Carcinoma: A Pilot Comparative Study. *Acad Radiol* 2015; **22**: 1344-1360 [PMID: 26211553 DOI: 10.1016/j.acra.2015.05.012]

54   **Donato H**, França M, Candelária I, Caseiro-Alves F. Liver MRI: From basic protocol to advanced techniques. *Eur J Radiol* 2017; **93**: 30-39 [PMID: 28668428 DOI: 10.1016/j.ejrad.2017.05.028]

55   **Brix G**, Griebel J, Kiessling F, Wenz F. Tracer kinetic modelling of tumour angiogenesis based on dynamic contrast-enhanced CT and

MRI measurements. *Eur J Nucl Med Mol Imaging* 2010; **37** Suppl 1: S30-S51 [PMID: 20503049 DOI: 10.1007/s00259-010-1448-7]

56   **Thng CH**, Koh TS, Collins DJ, Koh DM. Perfusion magnetic resonance imaging of the liver. *World J Gastroenterol* 2010; **16**: 1598-1609 [PMID: 20355238 DOI: 10.3748/wjg.v16.i13.1598]

57   **Sourbron S**. Technical aspects of MR perfusion. *Eur J Radiol* 2010; **76**: 304-313 [PMID: 20363574 DOI: 10.1016/j.ejrad.2010.02.017]

58   **Tofts PS**, Wicks DA, Barker GJ. The MRI measurement of NMR and physiological parameters in tissue to study disease process. *Prog Clin Biol Res* 1991; **363**: 313-325 [PMID: 1988983]

59   **Brix G**, Semmler W, Port R, Schad LR, Layer G, Lorenz WJ. Pharmacokinetic parameters in CNS Gd-DTPA enhanced MR imaging. *J Comput Assist Tomogr* 1991; **15**: 621-628 [PMID: 2061479]

60   **Larsson HB**, Stubgaard M, Frederiksen JL, Jensen M, Henriksen O, Paulson OB. Quantitation of blood-brain barrier defect by magnetic resonance imaging and gadolinium-DTPA in patients with multiple sclerosis and brain tumors. *Magn Reson Med* 1990; **16**: 117-131 [PMID: 2255233 DOI: 10.1002/mrm.1910160111]

61   **Abdullah SS**, Pialat JB, Wiart M, Duboeuf F, Mabrut JY, Bancel B, Rode A, Ducerf C, Baulieux J, Berthezene Y. Characterization of hepatocellular carcinoma and colorectal liver metastasis by means of perfusion MRI. *J Magn Reson Imaging* 2008; **28**: 390-395 [PMID: 18666145 DOI: 10.1002/jmri.21429]

62   **Szafer A**, Zhong J, Anderson AW, Gore JC. Diffusion-weighted imaging in tissues: theoretical models. *NMR Biomed* 1995; **8**: 289-296 [PMID: 8739267 DOI: 10.1002/nbm.1940080704]

63   **Taouli B**, Koh DM. Diffusion-weighted MR imaging of the liver. *Radiology* 2010; **254**: 47-66 [PMID: 20032142 DOI: 10.1148/radiol.09090021]

64   **Filipe JP**, Curvo-Semedo L, Casalta-Lopes J, Marques MC, Caseiro-Alves F. Diffusion-weighted imaging of the liver: usefulness of ADC values in the differential diagnosis of focal lesions and effect of ROI methods on ADC measurements. *MAGMA* 2013; **26**: 303-312 [PMID: 23053714 DOI: 10.1007/s10334-012-0348-1]

65   **Lim KS**. Diffusion-weighted MRI of hepatocellular carcinoma in cirrhosis. *Clin Radiol* 2014; **69**: 1-10 [PMID: 24034549 DOI: 10.1016/j.crad.2013.07.022]

66   **Sadowski EA**, Bennett LK, Chan MR, Wentland AL, Garrett AL, Garrett RW, Djamali A. Nephrogenic systemic fibrosis: risk factors and incidence estimation. *Radiology* 2007; **243**: 148-157 [PMID: 17267695 DOI: 10.1148/radiol.2431062144]

67   **Thomsen HS**, Marckmann P, Logager VB. Update on nephrogenic systemic fibrosis. *Magn Reson Imaging Clin N Am* 2008; **16**: 551-560, vii [PMID: 18926421 DOI: 10.1016/j.mric.2008.07.011]

68   **Takayama Y**, Nishie A, Asayama Y, Ishigami K, Kakihara D, Ushijima Y, Fujita N, Shirabe K, Takemura A, Honda H. Image quality and diagnostic performance of free-breathing diffusion-weighted imaging for hepatocellular carcinoma. *World J Hepatol* 2017; **9**: 657-666 [PMID: 28588750 DOI: 10.4254/wjh.v9.i14.657]

69   **Li X**, Li C, Wang R, Ren J, Yang J, Zhang Y. Combined Application of Gadoxetic Acid Disodium-Enhanced Magnetic Resonance Imaging (MRI) and Diffusion-Weighted Imaging (DWI) in the Diagnosis of Chronic Liver Disease-Induced Hepatocellular Carcinoma: A Meta-Analysis. *PLoS One* 2015; **10**: e0144247 [PMID: 26629904 DOI: 10.1371/journal.pone.0144247]

70   **Inchingolo R**, De Gaetano AM, Curione D, Ciresa M, Miele L, Pompili M, Vecchio FM, Giuliante F, Bonomo L. Role of diffusion-weighted imaging, apparent diffusion coefficient and correlation with hepatobiliary phase findings in the differentiation of hepatocellular carcinoma from dysplastic nodules in cirrhotic liver. *Eur Radiol* 2015; **25**: 1087-1096 [PMID: 25430005 DOI: 10.1007/s00330-014-3500-7]

71   **Briani C**, Di Pietropaolo M, Marignani M, Carbonetti F, Begini P, David V, Iannicelli E. Non-Hypervascular Hypointense Nodules at Gadoxetic Acid MRI: Hepatocellular Carcinoma Risk Assessment with Emphasis on the Role of Diffusion-Weighted Imaging. *J Gastrointest Cancer* 2017; Epub ahead of print [PMID: 28547117 DOI: 10.1007/s12029-017-9952-7]

72   **Xu PJ**, Yan FH, Wang JH, Lin J, Ji Y. Added value of breathhold diffusion-weighted MRI in detection of small hepatocellular carcinoma lesions compared with dynamic contrast-enhanced MRI alone using receiver operating characteristic curve analysis. *J Magn Reson Imaging* 2009; **29**: 341-349 [PMID: 19161186 DOI: 10.1002/jmri.21650]

73   **Jiang T**, Xu JH, Zou Y, Chen R, Peng LR, Zhou ZD, Yang M. Diffusion-weighted imaging (DWI) of hepatocellular carcinomas: a retrospective analysis of the correlation between qualitative and quantitative DWI and tumour grade. *Clin Radiol* 2017; **72**: 465-472 [PMID: 28109531 DOI: 10.1016/j.crad.2016.12.017]

74   **D'Amico F**, Schwartz M, Vitale A, Tabrizian P, Roayaie S, Thung S, Guido M, del Rio Martin J, Schiano T, Cillo U. Predicting recurrence after liver transplantation in patients with hepatocellular carcinoma exceeding the up-to-seven criteria. *Liver Transpl* 2009; **15**: 1278-1287 [PMID: 19790142 DOI: 10.1002/lt.21842]

75   **Sumie S**, Kuromatsu R, Okuda K, Ando E, Takata A, Fukushima N, Watanabe Y, Kojiro M, Sata M. Microvascular invasion in patients with hepatocellular carcinoma and its predictable clinicopathological factors. *Ann Surg Oncol* 2008; **15**: 1375-1382 [PMID: 18324443 DOI: 10.1245/s10434-008-9846-9]

76   **Yang C**, Wang H, Sheng R, Ji Y, Rao S, Zeng M. Microvascular invasion in hepatocellular carcinoma: is it predictable with a new, preoperative application of diffusion-weighted imaging? *Clin Imaging* 2017; **41**: 101-105 [PMID: 27840260 DOI: 10.1016/j.clinimag.2016.10.004]

77   **Gonzalez-Guindalini FD**, Botelho MP, Harmath CB, Sandrasegaran K, Miller FH, Salem R, Yaghmai V. Assessment of liver tumor response to therapy: role of quantitative imaging. *Radiographics* 2013; **33**: 1781-1800 [PMID: 24108562 DOI: 10.1148/rg.336135511]

78   **Heijmen L**, Ter Voert EE, Nagtegaal ID, Span P, Bussink J, Punt CJ, de Wilt JH, Sweep FC, Heerschap A, van Laarhoven HW. Diffusion-weighted MR imaging in liver metastases of colorectal cancer: reproducibility and biological validation. *Eur Radiol* 2013; **23**: 748-756 [PMID: 23001604 DOI: 10.1007/s00330-012-2654-4]

79   **Wagner M**, Doblas S, Daire JL, Paradis V, Haddad N, Leitão H, Garteiser P, Vilgrain V, Sinkus R, Van Beers BE. Diffusion-weighted MR imaging for the regional characterization of liver tumors. *Radiology* 2012; **264**: 464-472 [PMID: 22692032 DOI: 10.1148/radiol.12111530]

80   **Schraml C**, Schwenzer NF, Martirosian P, Bitzer M, Lauer U, Claussen CD, Horger M. Diffusion-weighted MRI of advanced hepatocellular carcinoma during sorafenib treatment: initial results. *AJR Am J Roentgenol* 2009; **193**: W301-W307 [PMID: 19770299 DOI: 10.2214/AJR.08.2289]

81   **Kamel IR**, Reyes DK, Liapi E, Bluemke DA, Geschwind JF. Functional MR imaging assessment of tumor response after 90Y microsphere treatment in patients with unresectable hepatocellular carcinoma. *J Vasc Interv Radiol* 2007; **18**: 49-56 [PMID: 17296704 DOI: 10.1016/j.jvir.2006.10.005]

82   **Bonekamp S**, Kamel I, Solga S, Clark J. Can imaging modalities diagnose and stage hepatic fibrosis and cirrhosis accurately? *J Hepatol* 2009; **50**: 17-35 [PMID: 19022517 DOI: 10.1016/j.jhep.2008.10.016]

83   **Venkatesh SK**, Yin M, Ehman RL. Magnetic resonance elastography of liver: technique, analysis, and clinical applications. *J Magn Reson Imaging* 2013; **37**: 544-555 [PMID: 23423795 DOI: 10.1002/jmri.23731]

84   **Thompson SM**, Wang J, Chandan VS, Glaser KJ, Roberts LR, Ehman RL, Venkatesh SK. MR elastography of hepatocellular carcinoma: Correlation of tumor stiffness with histopathology features-Preliminary findings. *Magn Reson Imaging* 2017; **37**: 41-45 [PMID: 27845245 DOI: 10.1016/j.mri.2016.11.005]

85   **Hennedige TP**, Hallinan JT, Leung FP, Teo LL, Iyer S, Wang G, Chang S, Madhavan KK, Wee A, Venkatesh SK. Comparison of magnetic resonance elastography and diffusion-weighted imaging for differentiating benign and malignant liver lesions. *Eur Radiol* 2016; **26**: 398-406 [PMID: 26032879 DOI: 10.1007/s00330-015-3835-8]

86   **Gordic S**, Ayache JB, Kennedy P, Besa C, Wagner M, Bane O,

Ehman RL, Kim E, Taouli B. Value of tumor stiffness measured with MR elastography for assessment of response of hepatocellular carcinoma to locoregional therapy. *Abdom Radiol* (NY) 2017; **42**: 1685-1694 [PMID: 28154910 DOI: 10.1007/s00261-017-1066-y]

87   **Li J**, Jamin Y, Boult JK, Cummings C, Waterton JC, Ulloa J, Sinkus R, Bamber JC, Robinson SP. Tumour biomechanical response to the vascular disrupting agent ZD6126 in vivo assessed by magnetic resonance elastography. *Br J Cancer* 2014; **110**: 1727-1732 [PMID: 24569471 DOI: 10.1038/bjc.2014.76]

88   **Pepin KM**, Chen J, Glaser KJ, Mariappan YK, Reuland B, Ziesmer S, Carter R, Ansell SM, Ehman RL, McGee KP. MR elastography derived shear stiffness--a new imaging biomarker for the assessment of early tumor response to chemotherapy. *Magn Reson Med* 2014; **71**: 1834-1840 [PMID: 23801372 DOI: 10.1002/mrm.24825]

89   **Gillies RJ**, Kinahan PE, Hricak H. Radiomics: Images Are More than Pictures, They Are Data. *Radiology* 2016; **278**: 563-577 [PMID: 26579733 DOI: 10.1148/radiol.2015151169]

90   **Rosenkrantz AB**, Pinnamaneni N, Kierans AS, Ream JM. Hypovascular hepatic nodules at gadoxetic acid-enhanced MRI: whole-lesion hepatobiliary phase histogram metrics for prediction of progression to arterial-enhancing hepatocellular carcinoma. *Abdom Radiol* (NY) 2016; **41**: 63-70 [PMID: 26830613 DOI: 10.1007/s00261-015-0610-x]

91   **Kim YK**, Lee WJ, Park MJ, Kim SH, Rhim H, Choi D. Hypovascular hypointense nodules on hepatobiliary phase gadoxetic acid-enhanced MR images in patients with cirrhosis: potential of DW imaging in predicting progression to hypervascular HCC. *Radiology* 2012; **265**: 104-114 [PMID: 22891358 DOI: 10.1148/radiol.12112649]

92   **Choi JW**, Lee JM, Kim SJ, Yoon JH, Baek JH, Han JK, Choi BI. Hepatocellular carcinoma: imaging patterns on gadoxetic acid-enhanced MR Images and their value as an imaging biomarker. *Radiology* 2013; **267**: 776-786 [PMID: 23401584 DOI: 10.1148/radiol.13120775]

93   **Kitao A**, Matsui O, Yoneda N, Kozaka K, Kobayashi S, Koda W, Gabata T, Yamashita T, Kaneko S, Nakanuma Y, Kita R, Arii S. Hypervascular hepatocellular carcinoma: correlation between biologic features and signal intensity on gadoxetic acid-enhanced MR images. *Radiology* 2012; **265**: 780-789 [PMID: 23175543 DOI: 10.1148/radiol.12120226]

94   **Zhou W**, Zhang L, Wang K, Chen S, Wang G, Liu Z, Liang C. Malignancy characterization of hepatocellular carcinomas based on texture analysis of contrast-enhanced MR images. *J Magn Reson Imaging* 2017; **45**: 1476-1484 [PMID: 27626270 DOI: 10.1002/jmri.25454]

Baishideng®